Action: respond to our copy-editing questions

Select each question and describe any changes we should make on the proof. Changes against journal style will not be made and proofs will not be sent back for further editing.

AQ1. Please check all author names and affiliations. Please check that author surnames have been identified by a pink background. This is to ensure that forenames and surnames have been correctly tagged for online indexing.

AQ2. If your manuscript has figures or text from other sources, please ensure you have permission from the copyright holder. For any questions about permissions contact jnls.author.support@oup.com.

AQ3. Please provide a Funding statement, detailing any funding received. Remember that any funding used while completing this work should be highlighted in a separate Funding section. Please ensure that you use the full official name of the funding body, and if your paper has received funding from any institution, such as NIH, please inform us of the grant number to go into the funding section. We use the institution names to tag NIH-funded articles so they are deposited at PMC.

AQ4. Please indicate if there is a conflict of interest, i.e. of a financial nature, although relevant non-financial disclosures can also be made.

AQ5. Please provide address lines for all the affiliations.

AQ6. Please note that reference “Fry et al. (1993)” is not listed in the reference list. Please add it to the list or delete the citation.

AQ7. Please clarify whether the in-text reference citation “Culbertson et al. (2016)” refers to “Culbertson et al. (2016a)” or “Culbertson et al. (2016b)”.

AQ8. Please consider rephrasing the sentence “This indirect assay measures UDP produced…” for clarity.

AQ9. Please check whether “34” in the sentence “Each cellohexaose molecule can accept…” refers to the reference “Pauly and Keegstra 2016”.

AQ10. Please clarify whether the in-text reference citation “Culbertson et al. (2016)” refers to “Culbertson et al. (2016a)” or “Culbertson et al. (2016b)”.

AQ11. Please clarify whether the in-text reference citation “Culbertson et al. (2016)” refers to “Culbertson et al. (2016a)” or “Culbertson et al. (2016b)”.

AQ12. Please spell out “HPAEC-PAD” in the sentence “HPAEC-PAD confirmed that digestion of glucocellohexaose…”.

AQ13. Please clarify whether the in-text reference citation “Culbertson et al. (2016)” refers to “Culbertson et al. (2016a)” or “Culbertson et al. (2016b)”.

AQ14. Please clarify whether the in-text reference citation “Culbertson et al. (2016)” refers to “Culbertson et al. (2016a)” or “Culbertson et al. (2016b)”.

AQ15. Please spell out “CSL” in the sentence “For example, the polysaccharides that have Glu…”.

AQ16. Please clarify whether the in-text reference citation “Culbertson et al. (2016)” refers to “Culbertson et al. (2016a)” or “Culbertson et al. (2016b)”.

AQ17. Please clarify whether the in-text reference citation “Culbertson et al. (2016)” refers to “Culbertson et al. (2016a)” or “Culbertson et al. (2016b)”.

AQ18. The setntence “The total protein concentration was determined…” is not clear. Please provide updated text.

AQ19. Please spell out “BSA” in the sentence “The total protein concentration was determined…”.

AQ20. The sentence “After 25 μL overnight XXT1 activity assay…” is not clear. Please provide updated text.

AQ21. Please provide the page range for the reference “Piqué et al., 2018”.

Action: check your manuscript information

Please check that the information in the table is correct. We use this information in the online version of your article and for sharing with third party indexing sites, where applicable.

Full affiliations Each unique affiliation should be listed separately; affiliations must contain only the applicable department, institution, city, territory, and country.	1Roy J. Carver Department of Biochemistry, Biophysics and Molecular Biology, Iowa State University, Ames, IA 50011, USA 2Graduate school, Department of Molecular Biology and Genetics, Cornell University, Ithaca, NY 14853, USA 3Department of Cell Biology, Harvard Medical School, Boston, MA 02115, USA
Group contributors The name of the group and individuals in this group should be given, if applicable (e.g. The BFG Working Group: Simon Mason, Jane Bloggs)	NA
Supplementary data files cited	**Supplementary data** are available at PCP online.
Funder Name(s) Please give the full name of the main funding body/agency. This should be the full name of the funding body without abbreviation or translation, if unsure, see https://search.crossref.org/funding	National Science Foundation- Plant Genome Research Program National Science Foundation Molecular and Cellular Biosciences

How to add your responses

These instructions show you how to add your responses to your proof using Adobe Acrobat Professional version 7 onwards, or Adobe Reader DC. To check what version you are using, go to 'Help', then 'About'. The latest version of Adobe Reader is available for free from https://get.adobe.com/uk/reader/.

Displaying the toolbars

Adobe Reader DC

In Adobe Reader DC, the Comment toolbar can be found by clicking 'Comment' in the menu on the top-right-hand side of the page (shown below).

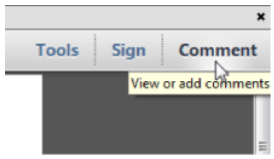

The toolbar shown below will then display along the right-hand-side of the page.

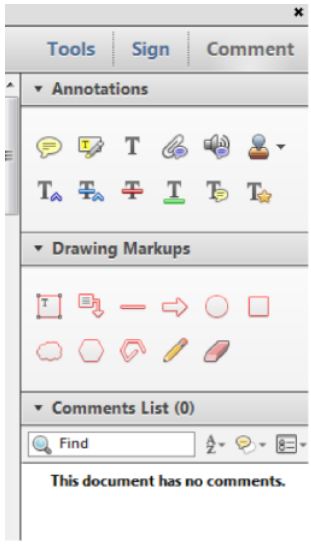

Acrobat Professional 7, 8 and 9

In Adobe Professional, the Comment toolbar can be found by clicking 'Comment(s)' in the top toolbar, and then clicking 'Show Comment & Markup Toolbar' (shown below).

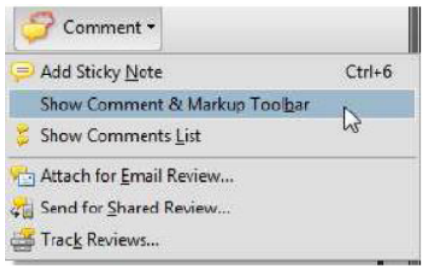

The toolbar shown below will then be displayed along the top of the page.

Using text edits and comments in Acrobat

This is the easiest method to both make changes, and for your changes to be transferred and checked.

1. Click 'Text Edits'
2. Select the text to be annotated or place your cursor at the insertion point and start typing.
3. Click the 'Text Edits' drop down arrow and select the required action.
4. You can also right click on selected text for a range of commenting options, or to add sticky notes.

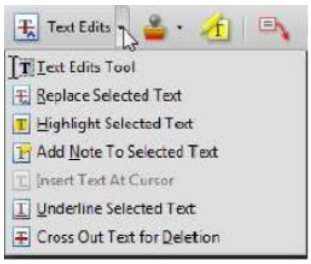

Using commenting tools in Adobe Reader

All commenting tools are displayed in the toolbar. You cannot use text edits, however you can still use highlighter, sticky notes, and a variety of insert/replace text options.

Pop-up notes

In both Reader and Acrobat, when you insert or edit text, a pop-up box will appear.

Saving comments

In order to save your comments and notes, you need to save the file ('File', 'Save') before closing the document.

NB: Do not make any edits directly into the text, use commenting tools only

PCP
PLANT & CELL PHYSIOLOGY

Special Issue – Regular Paper

Xyloglucan Xylosyltransferase 1 Displays Promiscuity Toward Donor Substrates During in Vitro Reactions

Jacqueline J. Ehrlich[1,2], Richard M. Weerts[1], Sayane Shome[1], Alan T. Culbertson[1,3], Richard B. Honzatko[1], Robert L. Jernigan[1] and Olga A. Zabotina[1,*]

[1]Roy J. Carver Department of Biochemistry, Biophysics and Molecular Biology, Iowa State University, Ames, IA 50011, USA
[2]Graduate school, Department of Molecular Biology and Genetics, Cornell University, Ithaca, NY 14853, USA
[3]Department of Cell Biology, Harvard Medical School, Boston, MA 02115, USA

*Corresponding author: E-mail, zabotina@iastate.edu

(Received 12 March 2021; Accepted 14 July 2021)

Glycosyltransferases (GTs) are a large family of enzymes that add sugars to a broad range of acceptor substrates, including polysaccharides, proteins and lipids, by utilizing a wide variety of donor substrates in the form of activated sugars. Individual GTs have generally been considered to exhibit a high level of substrate specificity, but this has not been thoroughly investigated across the extremely large set of GTs. Here we investigate xyloglucan xylosyltransferase 1 (XXT1), a GT involved in the synthesis of the plant cell wall polysaccharide, xyloglucan. Xyloglucan has a glucan backbone, with initial side chain substitutions exclusively composed of xylose from uridine diphosphate (UDP)-xylose. While this conserved substitution pattern suggests a high substrate specificity for XXT1, our in vitro kinetic studies elucidate a more complex set of behavior. Kinetic studies demonstrate comparable k_{cat} values for reactions with UDP-xylose and UDP-glucose, while reactions with UDP-arabinose and UDP-galactose are over 10-fold slower. Using k_{cat}/K_M as a measure of efficiency, UDP-xylose is 8-fold more efficient as a substrate than the next best alternative, UDP-glucose. To the best of our knowledge, we are the first to demonstrate that not all plant XXTs are highly substrate specific and some do show significant promiscuity in their in vitro reactions. Kinetic parameters alone likely do not explain the high substrate selectivity in planta, suggesting that there are additional control mechanisms operating during polysaccharide biosynthesis. Improved understanding of substrate specificity of the GTs will aid in protein engineering, development of diagnostic tools, and understanding of biological systems.

Keywords: Cell wall biosynthesis • Glycosyltransferase • Polysaccharide biosynthesis • Substrate specificity • Xyloglucan • Xyloglucan xylosyltransferase

Introduction

Xyloglucan (XyG) is a major hemicellulosic polysaccharide in the primary plant cell wall that is essential for normal growth and development. XyG was long thought to confer protective mechanical properties to the plant, but recent evidence suggests it is not needed for strength and may play various roles throughout the plant lifecycle (Kuki et al. 2020). XyG is most abundant in vascular, flowering plants (Perrin et al. 2003), but has also been detected in ferns, hornworts, liverworts, and mosses (Zabotina 2012). XyG has applications for biofuels, biomaterials, nutrition, cosmetics, and medicine (Mcdougall and Fry 1989, Larsbrink et al. 2014, Piqué et al. 2018). In addition to XyG, other branched polysaccharides with similar structures and substitutions may have industrial applications, so understanding and subsequently harnessing the process of polysaccharide synthesis lends itself to advances in materials science.

XXXG-type (Fry et al. (1993), has established simple XyG abbreviations to describe the substitution patterns found in various XyGs, with G for unsubstituted D-glucose, X for D-xylose, L for D-galactose, F for D-fucose, and S for L-arabinose. Branched polymers are named in the order of unsubstituted sugars. In XyG from *Arabidopsis thaliana* and other XXXG-type XyGs, the common motifs include XXXG, XXLG, XXFG and XLFG (Pauly et al. 2001, Obel et al. 2009)). XyG is synthesized by a Golgi-localized multiprotein complex (Chou et al. 2012, 2015) consisting of a glucan synthase and several glycosyltransferases (GTs; Ray 1980, Hayashi and Matsuda 1981, Chou et al. 2012). GTs are a superfamily of enzymes that glycosylate a wide variety of substrates including polysaccharides, proteins, lipids, nucleic acids and small molecules by adding a sugar moiety from an activated sugar donor, usually activated by a nucleotide or unsubstituted phosphate, to an acceptor substrate (Lairson et al. 2008). XyG is composed of a 1,4-β-linked glucan backbone decorated with 1,6-α-linked xylose residues, which are added by the GT, xyloglucan xylosyltransferase 1 (XXT1). Diversity among XyGs originates in the substitution patterns of the xylose residues added to the backbone and the GT-catalyzed extension of these xylose residues by other sugars such as galactose, fucose and arabinose (Zabotina 2012, Pauly and Keegstra 2016). Importantly, during the first step in XyG branching, XXTs always substitute

Plant Cell Physiol. 00(0): 1–12 (2021) doi:https://doi.org/10.1093/pcp/pcab114, Advance Access publication on xx xxx xxx, available online at https://academic.oup.com/pcp

native XyGs with xylose residues from UDP-xylose (UDP-Xyl) even though other UDP-sugars such as UDP-galactose (UDP-Gal), UDP-glucose (UDP-Glc) and UDP-arabinose (UDP-Ara) are present in the Golgi and can be utilized in subsequent synthesis steps (Carpita and Gibeaut 1993, Brett and Waldron 1996). While in planta, it seems logical that XXT1 would have a high substrate specificity for UDP-Xyl, our in vitro experimental evidence suggests otherwise.

In the plant GT superfamily as a whole, sugar donor selection is currently unresolved. The large number of plant GTs involved in polysaccharide biosynthesis and the high reproducibility of the polysaccharide structures they produce has suggested they perform with a high level of donor and acceptor substrate specificity. A few individual studies on plant glycosyltransferases have been performed, many for those involved in plant secondary metabolism. Of these, it has been suggested that donor substrate specificity may be controlled by the terminal domains of some specific GTs (Meech and Mackenzie 1997, Smith et al. 2020, Ross et al. 2001). For example, in a glucuronosyltransferase, the N-terminal half was proposed to be responsible for acceptor substrate specificity (Meech and Mackenzie 1997). According to a phylogenetic study, the C-terminal half of GTs could be involved in selecting donor substrates. (Ross et al. 2001, Smith et al. 2020). In contrast, the XXT1 crystal structure showed most donor substrate contacts are near the N-terminus, while the acceptor substrate has more contacts in the C-terminus (Culbertson et al. 2018). GT substrate specificity prediction based on amino acid sequence has also been investigated, particularly in highly conserved consensus sequences like the PSPG box of secondary metabolic proteins (Hughes and Hughes 1994, Jones et al. 1999, Vogt and Jones 2000, Kubo et al. 2004, Osmani et al. 2008). However, gene alignments have identified regions outside of these consensus sequences that are also involved in substrate specificity (Vogt and Jones 2000). Another study investigated a pectin-synthesizing enzyme, *At*GALS1, which was shown to be promiscuous for UDP-Gal and UDP-Ara in vitro and in vivo (Laursen et al. 2018). We were not able to find any other kinetic studies to show the extent of substrate specificity of plant-polysaccharide-synthesizing GTs.

XXT1 is a retaining GT with a GT-A fold involved in XyG synthesis in *Arabidopsis thaliana*. The XXT1 crystal structure revealed a mode of UDP binding similar to other GT structures (Lairson et al. 2008, Culbertson et al. 2018). Unique to XXT1 is the glucan chain acceptor substrate, which binds in a groove that allows xylose to be transferred to the sixth carbon (C6) hydroxyl group (Culbertson et al. 2018). XXT1 also contains a conserved glutamine residue that was proposed to be involved in the SN_i mechanism (Yu et al. 2015, Culbertson et al. 2018). Solving the structure of XXT1 has been a critical effort for understanding the mechanism of XyG biosynthesis (Culbertson et al. 2018), however a vital unanswered question remains—how does this machinery control the sequential selection of sugars during the synthesis of a complex polysaccharide in the plant Golgi? Here we present the first investigation into this unknown mechanism by investigating XXT donor substrate specificity. To this end, a set of alternative UDP-sugar substrates potentially present in the plant Golgi lumen are investigated. The soluble catalytic domain of XXT1, which has been recombinantly expressed and purified, was used to reveal the donor substrate promiscuity of XXT1 for the first time. Comparison of the kinetic parameters of XXT1 reactions with different sugars shows UDP-Xyl to be a preferred substrate but does not support the exclusive selectivity of XXT1 toward UDP-Xyl. Matrix-assisted laser desorption/ionization-time of flight (MALDI-TOF) analyses and enzymatic digestion of reaction products confirm XXT1's preferred substrate and its regiospecificity, showing that all donor substrates follow the same addition pattern. Computational modeling shows the similarities and differences between substrate fit in the XXT1 binding pocket. This study extends the conversation about substrate specificity of plant-polysaccharide-synthesizing GTs and offers promising directions in their applications.

Results

Assays for maximum UDP-sugar conversion and MALDI-TOF identification of products

XXT1 was expressed without a transmembrane domain in *Escherichia coli* cells and purified using Ni-NTA resin according to Culbertson et al. (2016). Protein extract from *E. coli* cells expressing an empty vector was passed through Ni-NTA column and was used as a negative control in all reactions (**Fig. 1A**). Screening of suitable XXT1 substrates (**Fig. 1A**) was carried out in 18-h reactions containing XXT1, a UDP-sugar, cellohexaose, Mn^{2+} and Tris-NaCl buffer (pH 7.4) in order to observe a maximum amount of donor substrate conversion to the glycosylated product. The reactions were allowed to proceed at room temperature, and the products were analyzed using the pyruvate kinase lactate dehydrogenase (PKLD) system (Gosselin et al. 1994). This indirect assay measures UDP produced in real time as a result of the sugar being added to the glucan backbone and UDP released as a second product. UDP is converted to uridine triphosphate and phosphoenolpyruvate is converted to pyruvate by pyruvate kinase. Pyruvate is then converted to lactate as nicotinamide adenine dinucleotide hydride (NADH) is converted to NAD+ and the loss of NADH can be monitored at absorbance 340 nm (**Supplementary Fig. S1**). Each cellohexaose molecule can accept up to three units of xylose[34]. The first addition of xylose is rapid and occurs on all cellohexaose molecules present in the solution before the addition of the second and third xyloses to the adjunct glucoses in the cellohexaose molecule (Cavalier and Keegstra 2006, Culbertson et al. 2016). Previously, in vitro studies demonstrated that most cellohexaose molecules are di-xylosylated, with some cellohexaose being tri-xylosylated after 18 h of the reaction (Culbertson et al. 2016). In this study, the reaction with cellohexaose at a concentration of 0.3 mM produces 0.7 mM of UDP, confirming previous results (**Fig. 1B**). Reactions using

Plant Cell Physiol. 00(0): 1–12 (2021) doi:https://doi.org/10.1093/pcp/pcab114

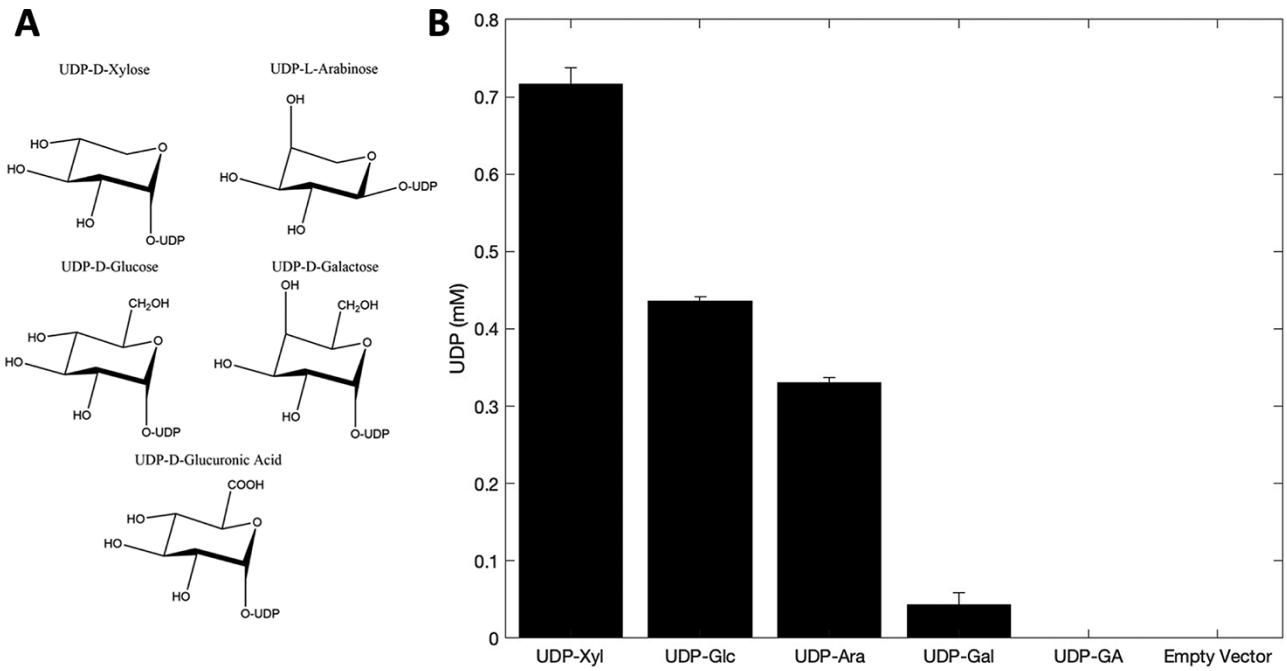

Fig. 1 (A) Chemical structures of UDP-sugars examined for XXT1 activity. (B) mM UDP produced as a result of transfer of sugar from UDP-sugar to cellohexaose after 18-h reactions. Each reaction contained 1 mM UDP-sugar and 0.3 mM cellohexaose. A control containing no cellohexaose was included as a baseline and was subtracted from all UDP values to account for any transfer of the sugar to water rather than to the glucan backbone. A reaction using an empty vector confirmed no activity for any remaining background proteins in the sample. Error bars represent standard deviation of triplicate reactions.

protein extract prepared from the cells expressing empty vector did not produce any detectable product. Products have been confirmed by MALDI-TOF mass spectrometry (MS) analyses (**Fig. 2A**).

To investigate the level of XXT1 specificity in vitro, we used other potential donor substrates using identical assay conditions as described above. XXT1 catalyzed reactions containing 1 mM UDP-Glc and 0.3 mM cellohexaose acceptor produced 0.4 mM UDP (**Fig. 1B**). This suggests that the main product of this reaction is mono-glucosylated cellohexaose, with a minor amount of di-glucosylated cellohexaose also present. This was confirmed by MALDI-TOF MS analysis of the products (**Fig. 2A**). Reactions with UDP-Ara and UDP-Gal produce 0.3 mM UDP and 0.04 mM UDP, respectively (**Fig. 1B**). Only one moiety of arabinose is added to all cellohexaose molecules in the reaction mixture (**Fig. 2A**). The reaction with UDP-Gal shows incomplete conversion of cellohexaose to mono-galactosylated cellohexaose; however, a significant amount of mono-galactosylated cellohexaose is produced (**Fig. 2A**). UDP-glucuronic acid (UDP-GlcA) was tested as a donor substrate, but no products were detected, so it was concluded that UDP-GlcA is not a suitable substrate for XXT1. Mannohexaose and mannan were tested as an alternative to the cellohexaose acceptor substrates in reactions with XXT1 using UDP-Xyl as a donor substrate, but neither of these reactions produce UDP (data not shown), which is consistent with previous studies (Faik et al. 2002). An empty vector control also did not show any activity.

Product digestion

The products of 18-h reactions were subjected to enzymatic digestion with β-glucosidase to determine the substitution patterns for each substrate according to a previous method by Cavalier and Keegstra (2006). β-glucosidase removes glucose units from the nonreducing end of the glucan backbone. If a glucose residue has been substituted, this enzyme cannot remove it.

Previous studies reported the first xylose addition at the fourth position from the reducing end produced GGXGGG[a], the second addition formed GGXXGG or GXXGGG, and the third addition formed GXXXGG (Cavalier and Keegstra 2006). Here, the MALDI results of the products after β-glucosidase digestion show peaks corresponding to XGGG, XXGG, XXGGG and XXXGG oligosaccharides (**Fig. 2B**). Because cellohexaose has six glucoses and unsubstituted glucoses are cleaved from the nonreducing end, these subunit sizes are derived from GGXGGG, GGXXGG, GXXGGG and GXXXGG reaction product motifs, which agrees with the previous study (Cavalier and Keegstra 2006).

Arabinocellohexaose, the other pentose, is added to a similar position on cellohexaose as xylose: because arabinocellohexaose was primarily mono-substituted during XXT1 reaction, this single arabinose is added to the fourth glucose in cellohexaose. After digestion of this product, only the SGGG fragment is detected (**Fig. 2B**). Reactions that contained glucose and those that contained galactose both had MALDI peaks

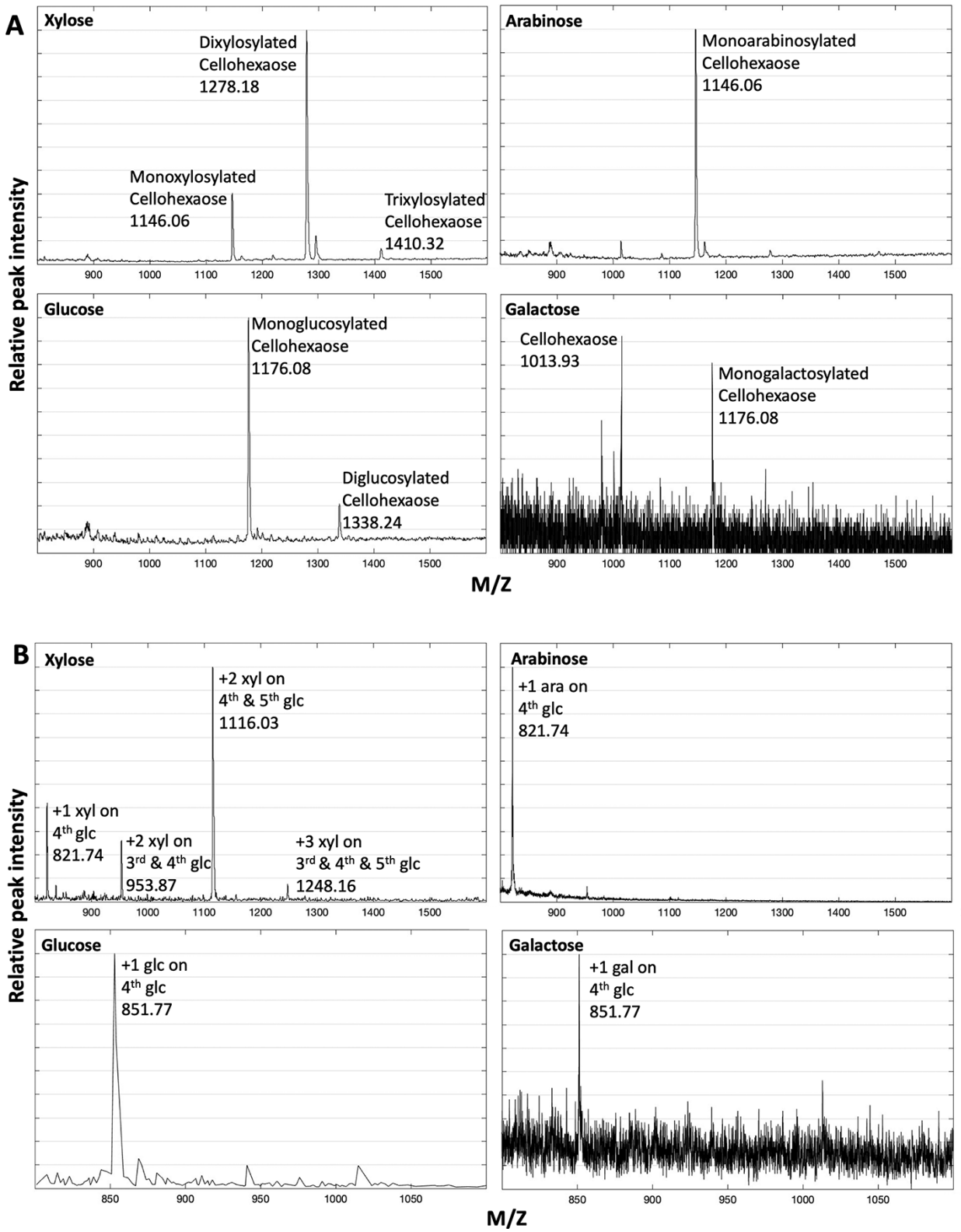

Fig. 2 (A) MALDI-TOF analysis of reaction products after 18-h reaction. Each sample was incubated in their respective UDP-sugar in a reaction identical to the 18-h reactions as described in **Fig. 1**. Products were precipitated with ethanol and resuspended in water before being added to a DHB matrix and subject to MALDI-TOF analysis by a Shimadzu AXIMA Confidence MALDI TOF Mass Spectrometer. Analysis was performed in linear mode at a power between 90 and 110 and pulse extraction of 1200, and 100 profiles were collected. Masses are reported with the addition of a sodium ion from the reaction buffer. (B) MALDI-TOF analysis of reaction products after 18-h digestion with β-glucosidase. β-glucosidase cleaves unsubstituted glucose molecules from the nonreducing end. Peaks are labeled by first specifying the number of side chain extensions followed by the position on the backbone which is numbered from the reducing end of cellohexaose.

Plant Cell Physiol. 00(0): 1–12 (2021) doi:https://doi.org/10.1093/pcp/pcab114

around 851.77, which likely corresponds to the addition of the sugar at the fourth glucose from the reducing end of cellohexaose (**Fig. 2B**). In these two last reactions, the moieties added to the backbone have the same masses as the glucoses within the backbone oligosaccharide, so it is difficult to determine whether the resulting molecules are linear chains of five moieties or branched tetrasaccharides with one moiety added as a branch. This peak could also be equivalent to a subunit with two sugars added at the second glucose in the backbone, but due to the low amount of di-glucosylated product and the lack of di-galactosylated product produced during 18-h reactions, this seems unlikely. HPAEC-PAD confirmed that digestion of glucocellohexaose was effectively complete since the peak corresponding to the cellohexaose internal standard disappeared. It also showed that glucose was being added to the backbone as a side chain extension, not as an extension of linear cellohexaose because the peak on the chromatogram obtained for the sample after β-glucosidase digestion shifted significantly smaller which, most likely, corresponds to the branched cellotetraose (**Supplementary Fig. S2**).

AQ12

Kinetic studies

The rate at which each sugar is added to the glucan backbone has been examined using an XXT assay coupled with a PKLD assay (Gosselin et al. 1994). The enzyme concentration was determined using a Bradford assay with absorbance at λ= 595 nm and then estimated based on band intensity. The reaction using 1.875 μM enzyme and UDP-Xyl exhibited a K_M of 3.6 ± 0.7 mM and a k_{cat} of 77.2 ± 0.1 min^{-1} (**Fig. 3**). The reaction with UDP-Glc and 1.875 μM enzyme exhibited a K_M of 21 ± 1 mM and a k_{cat} 53.39 ± 0.03 min^{-1} (**Fig. 3**), demonstrating donor substrate promiscuity of XXT1. The ability of XXT1 to accept UDP-Ara was assayed using 4 μM of enzyme, and calculations gave a K_M of 13 ± 1 mM and a k_{cat} of 3.93 ± 0.05 min^{-1} (**Fig. 3**). The reaction with UDP-Gal and 10 μM of enzyme exhibited a K_M of 66 ± 29 mM and a k_{cat} of 0.7 ± 0.3 min^{-1} (**Fig. 3**). Thus, the calculated kinetic efficiencies (k_{cat}/K_M) of UDP-Xyl, UDP-Glc, UDP-Ara and UDP-Gal were 21 ± 4 mM$^{-1} \cdot$ min^{-1}, 2.5 ± 0.2 mM$^{-1} \cdot$ min^{-1}, 0.30 ± 0.03 mM$^{-1} \cdot$ min^{-1} and 0.010 ± 0.006 mM$^{-1} \cdot$ min^{-1}, respectively.

In order to confirm the ability of XXT1 to accept UDP-Glc as a donor substrate, albeit at a higher K_M than UDP-Xyl, products of reactions containing both UDP-Xyl and UDP-Glc were examined using MALDI-TOF (**Fig. 4**). When the concentrations of the UDP-sugars were equivalent, there was a prominent monoxylosylation peak at *m*/*z* 1146.06 and a smaller peak corresponding to monoglucosylation at *m*/*z* 1176.08 (**Fig. 4A**). When the concentration of UDP-Glc was increased to three times that of the concentration of UDP-Xyl, the peaks corresponding to the masses of the xylosylated and glucosylated cellohexaose were nearly equivalent. Additionally, a small peak appeared at *m*/*z*

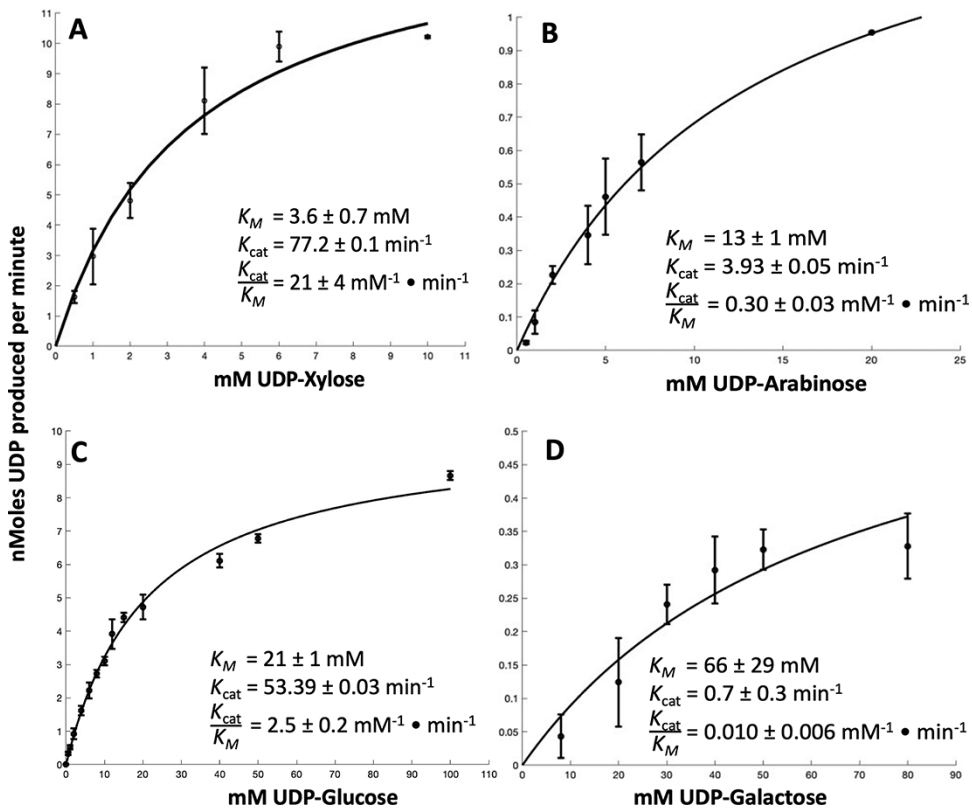

Fig. 3 Michaelis–Menten representations of enzyme kinetics of XXT1 using (A) UDP-xylose, (B) UDP-arabinose, (C) UDP-glucose (D) UDP-galactose and k_{cat} determined by nonlinear curve fitting. Error bars represent standard deviation of reactions performed in triplicate.

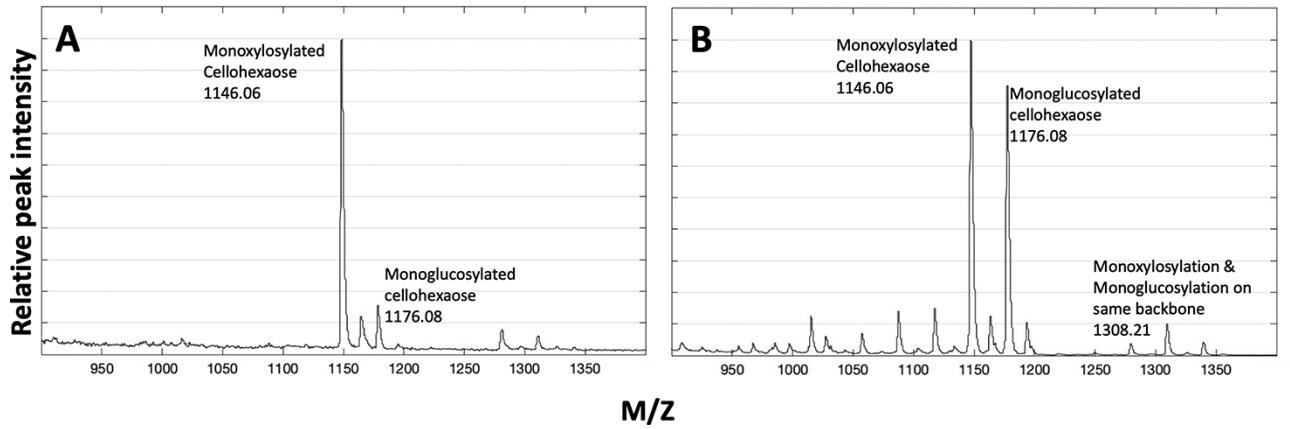

Fig. 4 MALDI-TOF analysis of 18-h reaction with (A) 1 mM UDP-Xyl and 1 mM UDP-Glc, and (B) 0.5 mM UDP-Xyl and 1.5 mM UDP-Glc. Apart from this change in sugar concentrations, assays were run as described in **Fig. 1**, and samples were prepared for MALDI-TOF as described in **Fig. 2**.

1308.21, which corresponds to the addition of one glucose and one xylose to the same molecule of cellohexaose (**Fig. 4B**).

Substrate modeling in the active site of XXT1

In a previous study we explored the conformation of UDP-xylose and its binding in the cavity of XXT1 with accessibility to the fourth carbon from the reducing end of cellohexaose and a Mn^{2+} ion, which is required for coordination with UDP-Xyl (Culbertson et al. 2018). Space in the cavity is limited, suggesting that UDP-xylose fits snugly into the conformation as shown (**Fig. 5D**). We have manually fit the other UDP-sugars tested in this study into that previously reported model of XXT1 (Culbertson et al. 2018), taking the analogous conformation of UDP-Xyl as a starting position; UDP-Ara, UDP-Glc and UDP-Gal were each manually aligned with UDP-Xyl in this conformation and then subject to energy minimization (**Fig. 5B**). The resulting UDP-sugars were all relatively easily accommodated; UDP-Ara, UDP-Glc and UDP-Gal had small root-mean-square deviations (RMSDs) of only 0.001, 0.3 and 0.3 Å, respectively, from the original UDP-Xyl. UDP-Ara is likely to have the smallest RMSD because it is the closest in structure to UDP-Xyl. None of the UDP-sugars have any collisions with other atoms in the structure. These nearly identical positions and orientations suggest a strong similarity in the binding poses for all four UDP-sugars used in the present study. Because of the easy acceptance of these UDP-sugars into the binding cavity, there was no need to make further efforts to develop the bound enzyme–substrate models.

Amino acid residues previously shown to be critical for enzymatic activity (Culbertson et al. 2018) were selected and the distances between these residues and each UDP-sugar was measured (**Fig. 5A**). Distance difference matrices (DDMs) were used to visualize the conformational changes between various atoms in the donor substrate and the active site residues of XXT1. Distances between two specific atoms were measured in each UDP-sugar and then subtracted from the corresponding distance in UDP-Xyl. Green cells represent an increase in distance, and red cells—a decrease. According to these calculations, UDP-Xyl binds most tightly in the active site in comparison to the other UDP-sugars (**Fig. 5C**). Examining the distances between the oxygen bridging the alpha and beta phosphates and the O5 in the UDP-Sugar, UDP-Xyl has a corresponding distance of 2.46 Å, while UDP-Ara, UDP-Glc and UDP-Gal have distances of 2.53, 2.60 and 2.60 Å, respectively. When looking at how differences in sugar substrates may affect access to the acceptor, the distances between C1 of each UDP-sugar and C6 of the fourth glucose in cellohexaose where the new sugar must be attached did not show significant differences for the donors used in this study; UDP-Xyl and UDP-Ara were approximately 4.9 Å apart and UDP-Glc and UDP-Gal were approximately 4.5 Å apart.

Although UDP-arabinofuranose (UDP-Ara*f*) is the most abundant form of UDP-Ara found in plants, only UDP-arabinopyranose (UDP-Ara*p*) was available to us for use in this study. UDP-Ara*p* is synthesized from either UDP-Xyl or the arabinose salvage pathway and is interconverted between UDP-Ara*p* and UDP-Ara*f* by UDP-Arabinopyranose mutase (Konishi et al. 2007, Bar-Peled and O'Neill 2011). It is generally assumed that because UDP-Ara*f* is the most abundant form, it would act as the nucleotide donor. However, Laursen et al. (2018) demonstrated that a pectin-synthesizing enzyme, *At*GALS1, which normally uses UDP-Gal as a substrate, not only utilizes UDP-Ara*p* in vivo and in vitro, but the enzyme cannot produce any detectable product with UDP-Ara*f* (Laursen et al. 2018). To entertain the notion that UDP-Ara*f* and UDP-Ara*p* may be accommodated differently in the active site of XXT1, we modeled UDP-Ara*f* into XXT1 and found no potential binding issues of UDP-Ara*f* with other amino acids in the active site (**Supplementary Fig. S4A–D**). The DDM profiles of UDP-Xyl and UDP-Ara*f* most closely matches with the profiles of UDP-Xyl and UDP-Ara*p*, not the other UDP-sugars (**Supplementary Fig. S4C**). Because the UDP-Xyl and UDP-Ara*f* profile has a few more patches of green than the other sugars indicating a contraction in the active site, it is possible that UDP-Ara*f* binds more tightly in the active site. The biggest differences in amino acid distances among UDP-Ara*p* and UDP-Ara*f* include

Plant Cell Physiol. 00(0): 1–12 (2021) doi:https://doi.org/10.1093/pcp/pcab114

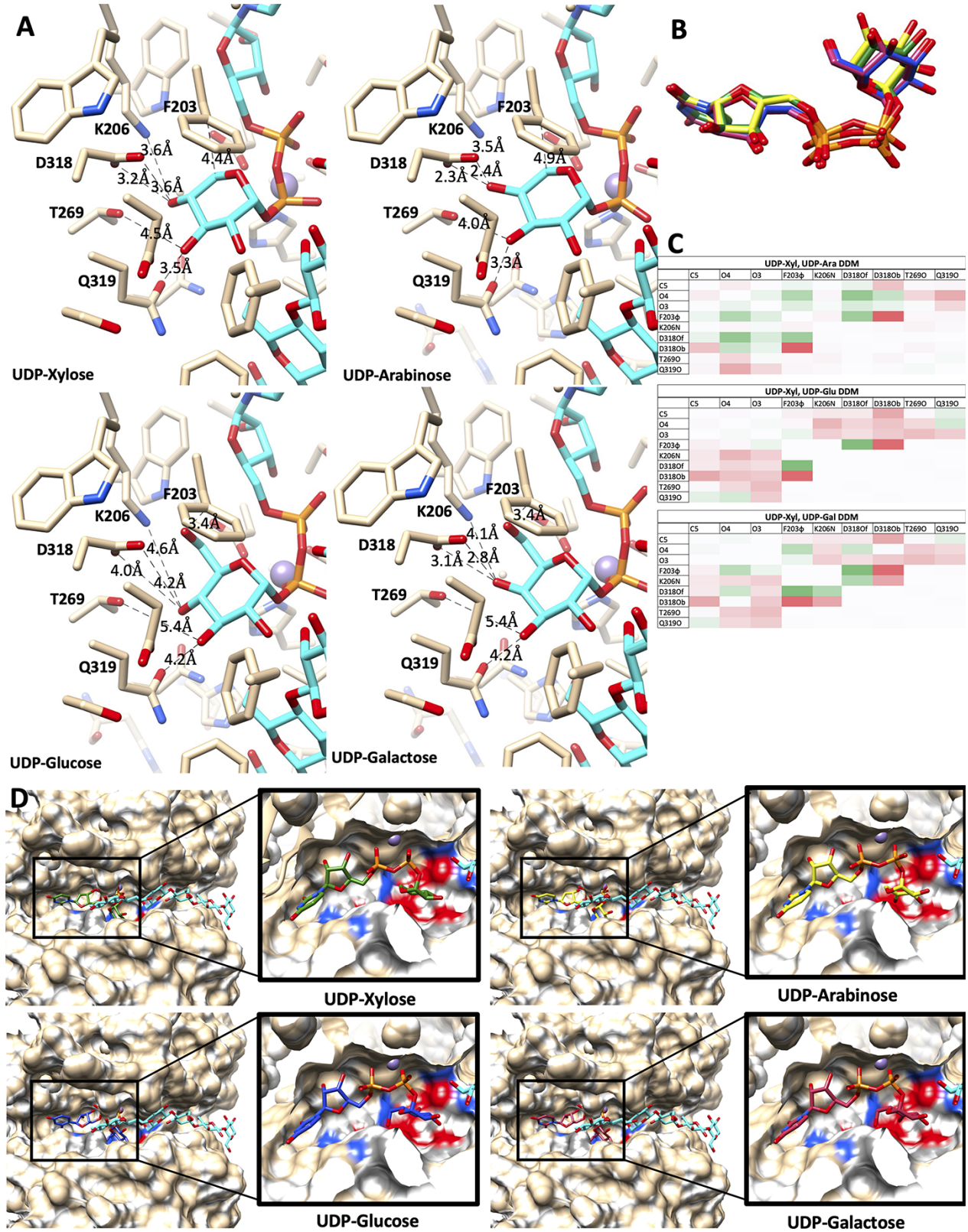

Fig. 5 (A) Modeling of each sugar substrate into the active site of XXT1 using previously docked UDP-Xyl as a template. Key catalytic residues are labeled and distances between each atom are reported in angstroms. (B) Superimposition of each UDP-sugar examined in this study. UDP-Xyl is shown in green, UDP-Ara is yellow, UDP-Glc is blue and UDP-Gal is magenta. (C) DDM representation of atomic distances between pairs of atoms in UDP-sugars subtracted from the same pairs of atoms in UDP-Xyl. A green box represents a positive distance difference between the atom pairs in UDP-Xyl minus the pairs in the other UDP-sugar, while a red box represents a negative difference. (D) Surface representation of the active site of XXT1 with each UDP-sugar substrate modeled into the binding cleft, which is in close proximity to the cellohexaose binding cleft. Colors are as noted in (B).

F203, which is further from the UDP-sugar in UDP-Ara*f* and K206, which is closer to the UDP-sugar in UDP-Ara*f*. While it is unclear how the changes between UDP-Ara*p* and UDP-Ara*f* could affect kinetics, we found no steric issues after energy minimization and conclude that UDP-Ara*f* could be relatively easily accommodated in the active site like the other sugars.

Discussion

In this study, we have shown that all four sugars are readily accepted by XXT1 as donor substrates and can be attached to a glucan backbone in vitro. However, in plants, the first sugars directly attached to the glucan backbone are exclusively xyloses, despite the presence of other nucleotide sugars in the Golgi lumen (Norambuena et al. 2002, Rollwitz et al. 2006, Handford et al. 2012, Rautengarten et al. 2014, 2017, Ebert et al. 2015, Khoder-Agha et al. 2019) and, thus, potentially available to XXTs during synthesis of XyG. In order to investigate the apparent discrepancy of XXTs specificities in the plant Golgi and their ability to accept other UDP-sugars in vitro, we have investigated XXT1 activity with five different nucleotide sugars by employing kinetics, MALDI-TOF analysis, and computational modeling.

In this study, the XXT1 enzyme was expressed in *E. coli*, purified, and assayed for activity following everything as reported in Culbertson et al. (2016). The k_{cat} of XXT1 with UDP-Xyl was previously reported to be 6.79 min^{-1} (Culbertson et al. 2016), whereas our results indicated XXT1 to be a much more efficient enzyme with a k_{cat} of 77.17 min^{-1}, although the calculated K_M in this study is higher in comparison to the previous estimation. The only difference between the current study and the previous one is how the products were measured. At this time, we do not have a clear-cut explanation of this difference in V_{max} and K_M observed for XXT1 in these two studies. Since K_M values could be impacted by the accuracy of V_{max} estimation, it is plausible to propose that the difference arises from the methods used for product quantification. In the previous study, HPAEC-PAD was used to quantify the production of xylosylated glucan oligosaccharides, which has an upper limit of substrate detection that could cause unintentional underestimation of xylosylated glucan after reactions with higher substrate concentrations. Such an underestimation of the final product can lead to a premature flattening of V_{max} curve followed by an underestimation of the V_{max} value, which would result in apparently lower K_M values. The upper limit of PKLD detection used in the current study can always be adjusted by the UDP standard curve used for quantification, so it does not have such rigid limitations in product quantification, and as a result, we did not observe such an abrupt saturation in the Menten curve as compared to the previous study. In addition, it is known that UDP can inhibit GT activity (Koster and Noordhoek 1983, Culbertson et al. 2016, Walia et al. 2018), which could also suppress the V_{max} in the previous study where both UDP and xylosylated glucan were accumulating. In the PKLD assay, UDP is used in the subsequent reaction for rate estimation. It is also notable that the K_M for XXT1 reported here is comparable to the K_M of 1.4 mM reported for IRX10-L, another xylosyltransferase (Urbanowicz et al. 2014). Regardless, all assays of the sugars were performed in parallel and used the same enzyme preparation, so we are still able to accurately assess the promiscuity of XXT1. Among the XXT1 reactions with different substrates, the kinetic parameters we unveiled may explain the enzyme's preferences for substrate selection in vivo. For example, the catalytic efficiencies of XXT1 reactions with UDP-Ara and UDP-Gal in comparison with UDP-Xyl are 70-fold and 2,000-fold lower, respectively. These differences indicate that UDP-Ara and UDP-Gal would need to be present in significantly higher concentrations in the Golgi lumen in order to compete with UDP-Xyl. On the other hand, XXT1 catalytic efficiency with UDP-Glc is only 8-fold lower in comparison with UDP-Xyl. In vitro, this difference in catalytic efficiency is not sufficient to prevent UDP-Glc additions altogether; UDP-Glc is able to compete with UDP-Xyl and can occasionally be added to the backbone when the concentrations are equivalent (**Fig. 4**). Two different products in equal amounts can be produced by increasing UDP-Glc only 3-fold in comparison with UDP-Xyl concentration, and the product with both xylose and glucose added to the glucan was also detected. Hence, if the concentrations of UDP-Xyl and UDP-Glc in the Golgi were comparable or there was an excess of UDP-Glc, this would result in some glucoses being occasionally attached to the glucan backbone of XyG instead of xyloses, but such a structure has never been detected in plant cell walls. One possibility is that the concentrations of UDP-Xyl and UDP-Glc in the Golgi lumen are not similar. Nucleotide sugar transporters (NSTs) for UDP-Xyl, UDP-Ara and UDP-Gal and to a lesser extent, UDP-Glc, have been identified in the Golgi, which may help understand which UDP-sugars may be present there (Norambuena et al. 2002, Rollwitz et al. 2006, Handford et al. 2012, Rautengarten et al. 2014, 2017, Ebert et al. 2015, Khoder-Agha et al. 2019). The XXT1 reaction with UDP-Glc has a significantly higher K_M than UDP-Xyl, so if there is a lower availability of UDP-Glc in the Golgi lumen, the UDP-Xyl would have significant preference as a donor substrate. This is the most likely scenario, given the lack of evidence suggesting that UDP-Glc is present in the Golgi lumen. For example, the polysaccharides that have Glc in their structures, such as mixed-linked glucans and glucomannans, are synthesized by CSL proteins which, most likely, have their active sites on the cytoplasmic side of the Golgi membrane (Kim et al. 2015), and furthermore glucomannan synthases use GDP-Glc rather than UDP-Glc (Liepman et al. 2005). Another possible explanation for the high substrate specificity of XXT1 in the Golgi is that GTs may also access UDP-sugars by forming complexes together with NSTs (Khoder-Agha et al. 2019), which could potentially provide UDP-sugars directly to the enzymes within the same complex. Although the association of any NST with the XyG-synthesizing enzymatic complex has not been investigated, the XyG-synthesizing complex could include a UDP-Xyl-specific transporter. Formation of such multiprotein complexes might also provide local conformational constraints that reduce GT promiscuity or increase the accessibility of selective substrates to active site of those GTs. There has not yet been

Plant Cell Physiol. 00(0): 1–12 (2021) doi:https://doi.org/10.1093/pcp/pcab114

any reported data on the abundance of each UDP-sugar in the Golgi, and there is no knowledge about their distribution within the *cis*, medial and *trans* Golgi. However, we cannot rule this out as a possible factor in substrate local availability for enzymes localized in different Golgi stacks.

UDP-Xyl and UDP-Ara are both pentoses and UDP-Glc and UDP-Gal are both hexoses, all having pyranose rings, with UDP-Glc and UDP-Gal carrying an additional hydroxymethyl on carbon 5 (**Fig. 1A**). In an earlier study of XXT1, UDP-Xyl had been manually fit into the active site of the crystal structure of *At*XXT1 with bound UDP using the conformation of UDP-Xyl from the structure of mouse xylosyltransferase (Culbertson et al. 2018). Here, all sugars were manually aligned to that UDP-Xyl-bound XXT1 model and distances between the sugar substrate and amino acids previously considered important for catalysis (Culbertson et al. 2018) were measured to learn which interactions would be better or worse (**Fig. 5A**). A steric clash between F203 and a C6 hydroxyl was previously thought to help distinguish between pentoses and hexoses (Culbertson et al. 2018), but according to our modeling that does not appear to be the case. The distances between C3 on each sugar and enzyme residues T269 and Q319 were nearly identical in each model, suggesting that these residues are more important for binding than catalysis. Contacts between the hydroxyl group on C4 and neighboring residues (D318 and K206) are suitable for interactions with UDP-Xyl and UDP-Glc, while the contacts for UDP-Ara and UDP-Gal are less than 2.4 and 2.8 Å, respectively. For UDP-Ara and UDP-Gal, the negative charge of D318 could result in repulsion in the active site, decreasing the ability for the sugars to bind and ultimately decreasing the enzymatic activity. The reaction using UDP-GlcA as a donor substrate did not produce any product, leading us to conclude that this UDP-sugar is not accepted by XXT1. The structure of UDP-GlcA is very similar to UDP-Glc, but the C6 carboxylic acid may cause steric clashes and electrostatic repulsion with the active site residue D318, preventing the binding of this sugar altogether. DDMs were used to illustrate conformational changes (**Fig. 5C**). While changes in kinetics cannot be directly correlated with distances between any one set of atoms, upon DDM analysis, it is clear that there are differences in the conformation of the enzyme when bound to different substrates. Interestingly, we observed shorter distances between the oxygen bridging the alpha and beta phosphates and the O5 in the UDP-sugar for UDP-Xyl compared to the other substrates, potentially correlating with a higher k_{cat}. We also evaluated donor substrate proximity to the acceptor substrate. With only a 0.4 Å difference between UDP-Xyl/UDP-Ara and UDP-Glc/UDP-Gal, we suggest that all UDP-sugars are positioned in the XXT1 active site in similar orientation, bringing their anomeric carbon to the acceptor carbon involved in the new covalent bond formation at similar proximities and, most likely, not contributing to the differences in kinetics observed for different UDP-sugars. This is in agreement with our previous MALDI-TOF analysis (**Fig. 2B**).

Previous studies have suggested that GTs are regiospecific (Hansen et al. 2003). In our study, MALDI-TOF analysis after 18-h assay shows that a majority of XXT1 xylosylation began on the fourth glucose from the reducing end of cellohexaose, which agrees with the regiospecificity reported in previous work (Cavalier and Keegstra 2006). Other sugars were added in a similar fashion, suggesting that the substrates bind similarly in the active site of XXT1. We did not investigate the type of new glycosidic linkage formed as a result of the reaction. But we assume that XXT1 acts as a retaining GT in all reactions because there is no residue that is positioned close enough to anomeric carbon in the donor to act as a nucleophile, which is required for SN_2 invertion mechanism (Culbertson et al. 2018). Additionally, the cellohexaose acceptor-binding site was essentially identical for each substrate in our models (data not shown). Cellohexaose is a chain of six glucose molecules, whereas mannohexaose is a chain of six mannose molecules. Glucose and mannose are epimers with the only difference at the second carbon; the C2 hydroxyl group in glucose is positioned equatorial down, while in mannose it is positioned axial up. To address the possible XXT1 promiscuity toward the acceptor substrate, mannohexaose and mannan were used in place of cellohexaose in the reactions with UDP-Xyl. Neither reaction produced any detectable product, in agreement with a previous study (Faik et al. 2002). These results could indicate that XXT1 has higher selectivity toward acceptor molecules in comparison with donor substrates; however, this will need to be investigated in more detail in the future using a larger set of possible oligosaccharides and considering all protein–acceptor interactions.

General patterns of substrate specificity of plant GTs remain unresolved due to their limited biochemical characterization. In this study, we demonstrated for the first time that XXT1, which had previously been regarded as having high substrate specificity, is instead able to accept a variety of UDP-sugars as donor substrates in vitro. Enzymatic assays producing the maximum product conversion, kinetic parameters of reactions using different UDP-sugars and computational modeling have all offered partial explanations as to why the glucan backbone in native XyG is always initially substituted with xylose residues and no other structures have been reported, despite the great diversity of nucleotide sugars available in the plant Golgi. The surprising substrate promiscuity of this plant GT raises interesting questions about the mechanisms controlling the high fidelity of complex polysaccharide structure synthesis in the plant Golgi and the substrate specificity of the GTs involved. The substrate promiscuity of XXT1 lends itself to interesting applications in materials science, through which designer polysaccharides could be synthesized, carrying branches of any sugar moiety accepted by XXT1. Given the large number of plant GTs, it is plausible that some others are also likely promiscuous, which could open the door for the synthesis of polysaccharides with virtually endless combinations of sugars, all synthesized by GTs.

Materials and Methods

Protein expression

A truncated version of *xxt1* lacking 22 amino acids in the putative transmembrane domain (Culbertson et al. 2016) was cloned into a pET20b vector with an N-terminal 6x-His tag and a protein G B1 domain (GB1) solubility tag as described in Culbertson et al. (2016). SoluBL21 *E. coli* cells containing the expression vector were grown at 37°C, while shaking at 200 rpm in 500 mL of Luria-Bertani (LB) growth media. After cells reached an optical density of 0.4 at 600 nm, the temperature was decreased to 18°C and protein expression was induced with the addition of 0.5 mM isopropyl β-D-1-thiogalactopyranoside. Expression was allowed to proceed at 18°C for 18 hs. Cells were pelleted at 6,000 *g* for 10 minutes. The pelleted cells were resuspended in 12.5 mL of 25 mM Tris-HCl (pH 7.4), 300 mM NaCl and 0.1 mM EDTA per 500 mL of LB growth media. Cells were flash frozen in liquid nitrogen for mechanical lysis. Cells were thawed and incubated with 1 mg lysozyme per 1 mL lysate at 4°C for 30 minutes. Final lysis via sonication was performed with an amplitude of 40 for 15-s pulses for a total of five times. The solubilized protein was isolated by centrifugation at 20,000 *g* for 30 minutes.

Protein purification

Crude lysate was purified using a nickel-nitrilotriacetic acid (Ni-NTA) column with a 1:10 (v/v) resin to lysate mixture. The mixture was incubated at 4°C for 1 h while rocking. The flow-through containing unbound protein and other small-molecule contaminants was discarded. The resin was washed four times with 8 mL of wash buffer containing 50 mM Tris-HCl (pH 7.4), 150 mM NaCl and 20 mM imidazole. XXT1 protein was eluted from the column using 8 mL of an elution buffer containing 50 mM Tris-HCl (pH 7.4), 150 mM NaCl and 300 mM imidazole. Protein was concentrated and buffer was changed to 150 mM NaCl and 50 mM Tris-HCl (pH 7.4) using 30K filtration tubes (Millipore-Sigma, UFC901024). As imidazole strongly affects XXT1 activity, protein was washed and filtered with approximately 4 mL 150/50 mM Tris-NaCl buffer (pH 7.4) after concentrating using the same 30K filtration tubes. Glycerol was added to the purified protein at a concentration of 20% (v/v) and stored at −80°C.

Protein quantification

Protein purity was estimated via sodium dodecylsulfate-polyacrylamide gel electrophoresis and Coomassie Blue G250 stain by observing the band purity. The total protein concentration was determined by Bradford assay using Quick Start Bradford Dye reagent 1X (Biorad 500-0205) and absorbance at 595 nm with a BSA standard curve, then was estimated based on band intensity.

Maximum sugar conversion assays

Assays were incubated in 75 mM NaCl, 50 mM Tris-HCl (pH 7.4), 1 mM UDP-sugar (UDP-Xyl, UDP-Ara Carbosource services; UDP-Glc, UDP-Gal Sigma-Aldrich 117756-22-6 and 137868-52-1), 0.3 mM cellohexaose (Megazyme, O-CHE), 0.5 mM $MnCl_2$ and 4.5 μM XXT1 enzyme for 18 h at 25°C while shaking at 180 rpm. Assays were performed in triplicate in 50-μL reaction volumes where 25 μL of reaction was used for pyruvate kinase lactate dehydrogenase (PKLD; Sigma-Aldrich P0294) detection and the remainder was purified for MALDI-TOF analysis.

XXT1 product purification

After 25 μL overnight XXT1 activity assay had been removed for UDP quantification, the remainder was purified and xylosylated cellohexaose was assessed with MALDI-TOF. To purify, the solution was incubated in 900 μL of 100% ethanol at −20°C overnight. Afterward, it was centrifuged at 21,000 *g* for 30 minutes and the supernatant was removed. The pellet was resuspended in water and centrifuged at 21,000 *g* again. The resulting supernatant was used for analysis in triplicate.

Glucosidase treatment

After the reactions proceeded for 18 h, the reactants were digested with β-glucosidase (Megazyme, E-BGLUC) to determine which position on the backbone they were added according to Cavalier and Keegstra (2006). Samples were spiked with 0.3 μM cellohexaose to use as an internal standard, insuring complete digestion. Samples were dried and then resuspended in 25 mM sodium acetate. Fifty milliunits of β-glucosidase was added to the sample and the reaction was proceeded at 37°C overnight. The reaction was terminated by heating at 100°C for 10 minutes. The sample was centrifuged at 14,000 × g for 5 minutes and 25 μL of supernatant was analyzed with MALDI. Reaction was carried out in triplicate.

MALDI-TOF analysis

A MALDI-TOF plate (Kratos Analytical) was spotted with equal volumes of purified product sample and 10 mg/mL 2,5-dihydroxybenzoic acid (DHB) matrix. The Shimadzu AXIMA Confidence MALDI TOF Mass Spectrometer was calibrated using 1 mg/mL of adrenocorticotropic hormone fragment 18–39 human (Sigma-Aldrich, A0673) and equal volumes of DHB matrix. The spots were allowed to dry overnight before MALDI-TOF analysis. Samples were analyzed in linear mode. Laser power was set at 100 mV and 100 profiles were collected for each run.

HPAEC-PAD

Glucocellohexoase was digested with β-glucosidase to further confirm the addition of glucose onto the cellohexaose backbone. Glucocellohexaose was digested according to β-glucosidase treatment. As described above, the digestion reactions were spiked with cellohexaose to ensure the completeness of digestion. One digestion mixture was not spiked with additional cellohexaose to distinguish the peaks corresponding to glucosylated cellohexaose and cellohexaose in the same reaction mixture. Products obtained from the enzymatic activity assays and after β-glucosidase digestion were analyzed by HPAEC with a pulsed amperometric detector (Dionex), as described previously (Cavalier and Keegstra 2006). The reaction mixtures were boiled for 10 min and centrifuged to precipitate denatured enzymes. The aliquots of the supernatants were injected onto a CarboPac PA-20 column and eluted using the following gradient: 0–80 mM of sodium acetate for 40 min, with 100 mM NaOH remaining constant through the entire run; after the 40-min run, the column was re-equilibrated for 15 min to the initial conditions.

XXT1 kinetic activity assays

Kinetics assays were coupled to a PKLD detection assay and performed in a 96-well plate. Assays had a total volume of 100 μL and contained 150 mM NaCl, 50 mM Tris-HCl (pH 7.4), 1 mM cellohexaose, 3 mM $MnCl_2$, 1.875 μM XXT1 enzyme, 2 μL PKLD mix (Sigma-Aldrich, P0294), 1.2 mM NADH (Fisher, PI88018) and 1 mM PEP (Fisher, AAB2035806). The reaction was initiated by the addition of XXT1 and PKLD enzymes and an initial velocity progress curve was immediately measured at 340 nm using a Biotek plate reader. PKLD enzymes were added to the reaction mixture first in order to burn off any UDP contaminant. Assays with varying concentrations of PKLD enzymes were performed to ensure that XXT1 catalysis is the rate-limiting step, and the initial velocity was shown to increase linearly with XXT1 concentration.

The conversion of NADH to NAD+ was monitored for 5–10 minutes at 340 nm to determine the initial velocity. The stoichiometry for the coupled reaction is 1:1:1, so the rate of NADH consumption is proportional to the rate of UDP production, which is proportional to the rate of sugar addition to the backbone. The results of control reactions without cellohexaose were subtracted from the initial velocity measurements to account for any background reactions

due to the presence of free UDP in UDP-sugar samples. Assays were performed in triplicate.

Manual alignment of sugars

UDP-Xyl was previously modeled into the XXT1 active site by using a homolog as described previously (Culbertson et al. 2018). The chemical structures of the remaining three UDP-sugars were obtained from the Pubchem database (CID: 3082070, CID: 8629 and CID:18068) and were manually aligned to UDP-Xyl. After the manual alignment, the structures were subjected to minimization using the Yasara server (Krieger et al. 2009).

Supplementary Data

Supplementary data are available at PCP online.

Data availability

All data underlying this article are available in the article and in its online supplementary material.

Funding

National Science Foundation Molecular and Cellular Biosciences (grant 1856477, 2019-2023) to O.A.Z, R.L.J. and R.B.H; National Science Foundation-Plant Genome Research Program (grant 1951819 2020-2023) to O.A.Z..

Disclosures

The authors have no conflicts of interest to declare.

References

Bar-Peled, M. and O'Neill, M. A. (2011) Plant nucleotide sugar formation, interconversion, and salvage by sugar recycling. *Annu. Rev. Plant Biol.* 62: 127–155.

Brett, C. T. and Waldron, K. W. (1996) Physiology and Biochemistry of Plant Cell Walls. Springer, Dordrecht.

Carpita, N. C. and Gibeaut, D. M. (1993) Structural models of primary cell walls in flowering plants: consistency of molecular structure with the physical properties of the walls during growth. *Plant J.* 3: 1–30.

Cavalier, D. M. and Keegstra, K. (2006) Two xyloglucan xylosyltransferases catalyze the addition of multiple xylosyl residues to cellohexaose. *J. Biol. Chem.* 281: 34197–34207.

Chou, Y.-H., Pogorelko, G., Young, Z. T. and Zabotina, O. A. (2015) Protein–protein interactions among xyloglucan-synthesizing enzymes and formation of Golgi-localized multiprotein complexes. *Plant Cell Physiol.* 56: 255–267.

Chou, Y.-H., Pogorelko, G. and Zabotina, O. A. (2012) Xyloglucan Xylosyltransferases XXT1, XXT2, and XXT5 and the glucan synthase CSLC4 form golgi-localized multiprotein complexes. *Plant Physiol.* 159: 1355–1366.

Culbertson, A. T., Chou, Y.-H., Smith, A. L., Young, Z. T., Tietze, A. A., Cottaz, S., Fauré, R. and Zabotina, O. A. (2016a) Enzymatic activity of xyloglucan xylosyltransferase 5. *Plant Physiol.* 171: 1893–1904.

Culbertson, A. T., Ehrlich, J. J., Choe, J.-Y., Honzatko, R. B. and Zabotina, O. A. (2018) Structure of xyloglucan xylosyltransferase 1 reveals simple steric rules that define biological patterns of xyloglucan polymers. *Proc. Natl. Acad. Sci. USA* 115: 6064–6069.

Culbertson, A. T., Smith, A. L., Cook, M. D. and Zabotina, O. A. (2016b) Truncations of xyloglucan xylosyltransferase 2 provide insights into the roles of the N- and C-terminus. *Phytochemistry* 128: 12–19.

Ebert, B., Rautengarten, C., Guo, X., Xiong, G., Stonebloom, S., Smith-Moritz, A. M., Herter, T., Chan, L. J. G., Adams, P. D., Petzold, C. J., Pauly, M., Willats, W. G. T., Heazlewood, J. L. and Scheller, H. V. (2015) Identification and characterization of a Golgi-localized UDP-xylose transporter family from Arabidopsis. *Plant Cell* 27: 1218–1227.

Faik, A., Price, N. J., Raikhel, N. V. and Keegstra, K. (2002) An Arabidopsis gene encoding an alpha-xylosyltransferase involved in xyloglucan biosynthesis. *Proc. Natl. Acad. Sci. USA* 99: 7797–7802.

Gosselin, S., Alhussaini, M., Streiff, M. B., Takabayashi, K. and Palcic, M. M. (1994) A continuous spectrophotometric assay for glycosyltransferases. *Anal. Biochem.* 220: 92–97.

Handford, M., Rodríguez-Furlán, C., Marchant, L., Segura, M., Gómez, D., Alvarez-Buylla, E., Xiong, G.-Y., Pauly, M. and Orellana, A. (2012) Arabidopsis thaliana AtUTr7 encodes a golgi-localized UDP–Glucose/UDP–galactose transporter that affects lateral root emergence. *Mol. Plant* 5: 1263–1280.

Hansen, K. S., Kristensen, C., Tattersall, D. B., Jones, P. R., Olsen, C. E., Bak, S. and Møller, B. L. (2003) The in vitro substrate regiospecificity of recombinant UGT85B1, the cyanohydrin glucosyltransferase from Sorghum bicolor. *Phytochemistry* 64: 143–151.

Hayashi, T. and Matsuda, K. (1981) Biosynthesis of xyloglucan in suspension-cultured soybean cells. An assay method for xyloglucan xylosyltransferase and attempted synthesis of xyloglucan from UDP-D-xylose. *J. Biochem.* 89: 325–328.

Hughes, J. and Hughes, M. A. (1994) Multiple secondary plant product UDP-glucose glucosyltransferase genes expressed in cassava (Manihot esculenta Crantz) cotyledons. *DNA Sequence* 5: 41–49.

Jones, P. R., Moller, B. L. and Hoj, P. B. (1999) The UDP-glucose: p-hydroxymandelonitrile-O-glucosyltransferasethat catalyzes the last step in synthesis of the cyanogenic glucoside dhurrin in Sorghum bicolor. Isolation, cloning, heterologous expression, and substrate specificity. *J. Biol. Chem.* 274: 35483–35491.

Khoder-Agha, F., Sosicka, P., Escriva Conde, M., Hassinen, A., Glumoff, T., Olczak, M. and Kellokumpu, S. (2019) N-acetylglucosaminyltransferases and nucleotide sugar transporters form multi-enzyme–multi-transporter assemblies in golgi membranes in vivo. *Cell. Mol. Life Sci.* 76: 1821–1832.

Kim, S.-J., Zemelis, S., Keegstra, K. and Brandizzi, F. (2015) The cytoplasmic localization of the catalytic site of CSLF6 supports a channeling model for the biosynthesis of mixed-linkage glucan. *Plant J.* 81: 537–547.

Konishi, T., Takeda, T., Miyazaki, Y., Ohnishi-Kameyama, M., Hayashi, T., O'Neill, M. A. and Ishii, T. (2007) A plant mutase that interconverts UDP-arabinofuranose and UDP-arabinopyranose. *Glycobiology* 17: 345–354.

Koster, A. S. and Noordhoek, J. (1983) Kinetic properties of the rat intestinal microsomal 1-naphthol: UDP-glucuronosyl transferase: inhibition by UDP and UDP-N-acetylglucosamine. *Biochim. Biophy. Acta (BBA)* 761: 76–85.

Krieger, E., Joo, K., Lee, J., Lee, J., Raman, S., Thompson, J., Tyka, M., Baker, D. and Karplus, K. (2009) Improving physical realism, stereochemistry, and side-chain accuracy in homology modeling: four approaches that performed well in CASP8. *Proteins* 77: 114–122.

Kubo, A., Arai, Y., Nagashima, S. and Yoshikawa, T. (2004) Alteration of sugar donor specificities of plant glycosyltransferases by a single point mutation. *Arch. Biochem. Biophys.* 429: 198–203.

Kuki, H., Yokoyama, R., Kuroha, T. and Nishitani, K. (2020) Xyloglucan is not essential for the formation and integrity of the cellulose network in the primary cell wall regenerated from Arabidopsis Protoplasts. *Plants* 9: 629.

Lairson, L. L., Henrissat, B., Davies, G. J. and Withers, S. G. (2008) Glycosyltransferases: structures, functions, and mechanisms. *Annu. Rev. Biochem.* 77: 521–555.

Larsbrink, J., Rogers, T. E., Hemsworth, G. R., McKee, L. S., Tauzin, A. S., Spadiut, O., Klinter, S., Pudlo, N. A., Urs, K., Koropatkin, N. M., Creagh, A. L., Haynes, C. A., Kelly, A. G., Cederholm, S. N., Davies, G. J., Martens, E. C. and Brumer, H. (2014) A discrete genetic locus confers xyloglucan metabolism in select human gut Bacteroidetes. *Nature* 506: 498–502.

Laursen, T., Stonebloom, S. H., Pidatala, V. R., Birdseye, D. S., Clausen, M. H., Mortimer, J. C. and Scheller, H. V. (2018) Bifunctional glycosyltransferases catalyze both extension and termination of pectic galactan oligosaccharides. *Plant J.* 94: 340–351.

Liepman, A. H., Wilkerson, C. G. and Keegstra, K. (2005) Expression of cellulose synthase-like (Csl) genes in insect cells reveals that CslA family members encode mannan synthases. *Proc. Natl. Acad. Sci. USA* 102: 2221–2226.

Mcdougall, G. J. and Fry, S. C. (1989) Anti-auxin activity of xyloglucan oligosaccharides: the rôle of groups other than the terminal α-L-fucose residue. *J. Exp. Bot.* 40: 233–238.

Meech, R. and Mackenzie, P. I. (1997) Structure and function of uridine diphosphate glucuronosyltransferases. *Clin. Exp. Pharmacol. Physiol.* 24: 907–915.

Norambuena, L., Marchant, L., Berninsone, P., Hirschberg, C. B., Silva, H. and Orellana, A. (2002) Transport of UDP-galactose in Plants. Identification and functional characterization of AtUTr1, an Arabidopsis Thaliana UDP-galactose/UDP-glucose transporter. *J. Biol. Chem.* 277: 32923–32929.

Obel, N., Erben, V., Schwarz, T., Kühnel, S., Fodor, A. and Pauly, M. (2009) Microanalysis of plant cell wall polysaccharides. *Mol. Plant* 2: 922–932.

Osmani, S. A., Bak, S., Imberty, A., Olsen, C. E. and Møller, B. L. (2008) Catalytic key amino acids and UDP-sugar donor specificity of a plant glucuronosyltransferase, UGT94B1: molecular modeling substantiated by site-specific mutagenesis and biochemical analyses. *Plant Physiol.* 148: 1295–1308.

Pauly, M. and Keegstra, K. (2016) Biosynthesis of the plant cell wall matrix polysaccharide xyloglucan. *Annu. Rev. Plant Biol.* 67: 235–259.

Pauly, M., Qin, Q., Greene, H., Albersheim, P., Darvill, A. and York, W. S. (2001) Changes in the structure of xyloglucan during cell elongation. *Planta* 212: 842–850.

Perrin, R. M., Jia, Z., Wagner, T. A., O'Neill, M. A., Sarria, R., York, W. S., Raikhel, N. V. and Keegstra, K. (2003) Analysis of xyloglucan fucosylation in Arabidopsis. *Plant Physiol.* 132: 768–778.

Piqué, N., Gómez-Guillén, M. Del C. and Montero, M. P. (2018) Xyloglucan, a plant polymer with barrier protective properties over the mucous membranes: an overview. *Int. J. Mol. Sci.* 19.

Rautengarten, C., Birdseye, D., Pattathil, S., McFarlane, H. E., Saez-Aguayo, S., Orellana, A., Persson, S., Hahn, M. G., Scheller, H. V., Heazlewood, J. L. and Ebert, B. (2017) The elaborate route for UDP-arabinose delivery into the Golgi of plants. *Proc. Natl. Acad. Sci. USA* 114: 4261–4266.

Rautengarten, C., Ebert, B., Moreno, I., Temple, H., Herter, T., Link, B., Doñas-Cofré, D., Moreno, A., Saéz-Aguayo, S., Blanco, F., Mortimer, J. C., Schultink, A., Reiter, W.-D., Dupree, P., Pauly, M., Heazlewood, J. L., Scheller, H. V. and Orellana, A. (2014) The Golgi localized bifunctional UDP-rhamnose/UDP-galactose transporter family of Arabidopsis. *Proc. Natl. Acad. Sci. USA* 111: 11563–11568.

Ray, P. M. (1980) Cooperative action of β-glucan synthetase and UDP-xylose xylosyl transferase of Golgi membranes in the synthesis of xyloglucan-like polysaccharide. *Biochim. Biophy. Acta (BBA)* 629: 431–444.

Rollwitz, I., Santaella, M., Hille, D., Flügge, U.-I. and Fischer, K. (2006) Characterization of AtNST-KT1, a novel UDP-galactose transporter from Arabidopsis thaliana. *FEBS Lett.* 580: 4246–4251.

Ross, J., Li, Y., Lim, E.-K. and Bowles, D. J. (2001) Higher Plant Glycosyltransferases. *Genome Biol.* 2: 3004.1–3004.6.

Smith, A. D., Page, B. D. G., Collier, A. C. and Coughtrie, M. W. H. (2020) Homology modeling of human uridine-5′-diphosphate-glucuronosyltransferase 1A6 reveals insights into factors influencing substrate and cosubstrate binding. *ACS Omega* 5: 6872–6887.

Urbanowicz, B. R., Peña, M. J., Moniz, H. A., Moremen, K. W. and York, W. S. (2014) Two Arabidopsis proteins synthesize acetylated xylan in vitro. *Plant J.* 80: 197–206.

Vogt, T. and Jones, P. (2000) Glycosyltransferases in plant natural product synthesis: characterization of a supergene family. *Trends Plant Sci.* 5: 380–386.

Walia, G., Smith, A. D., Riches, Z., Collier, A. C. and Coughtrie, M. W. H. (2018) The effects of UDP-sugars, UDP and Mg2+on uridine diphosphate glucuronosyltransferase activity in human liver microsomes. *Xenobiotica* 48: 882–890.

Yu, H., Takeuchi, M., LeBarron, J., Kantharia, J., London, E., Bakker, H., Haltiwanger, R. S., Li, H. and Takeuchi, H. (2015) Notch-modifying xylosyltransferase structures support an S N i-like retaining mechanism. *Nat. Chem. Biol.* 11: 847–854.

Zabotina, O. A. (2012) Xyloglucan and its biosynthesis. *Front. Plant Sci.* 3: 134.

AQ21